

Supplemental Data

Supplemental Tables

Supplemental Table 1: Combinations of iterations and subsets used for each total OSEM updates in Flash3d.

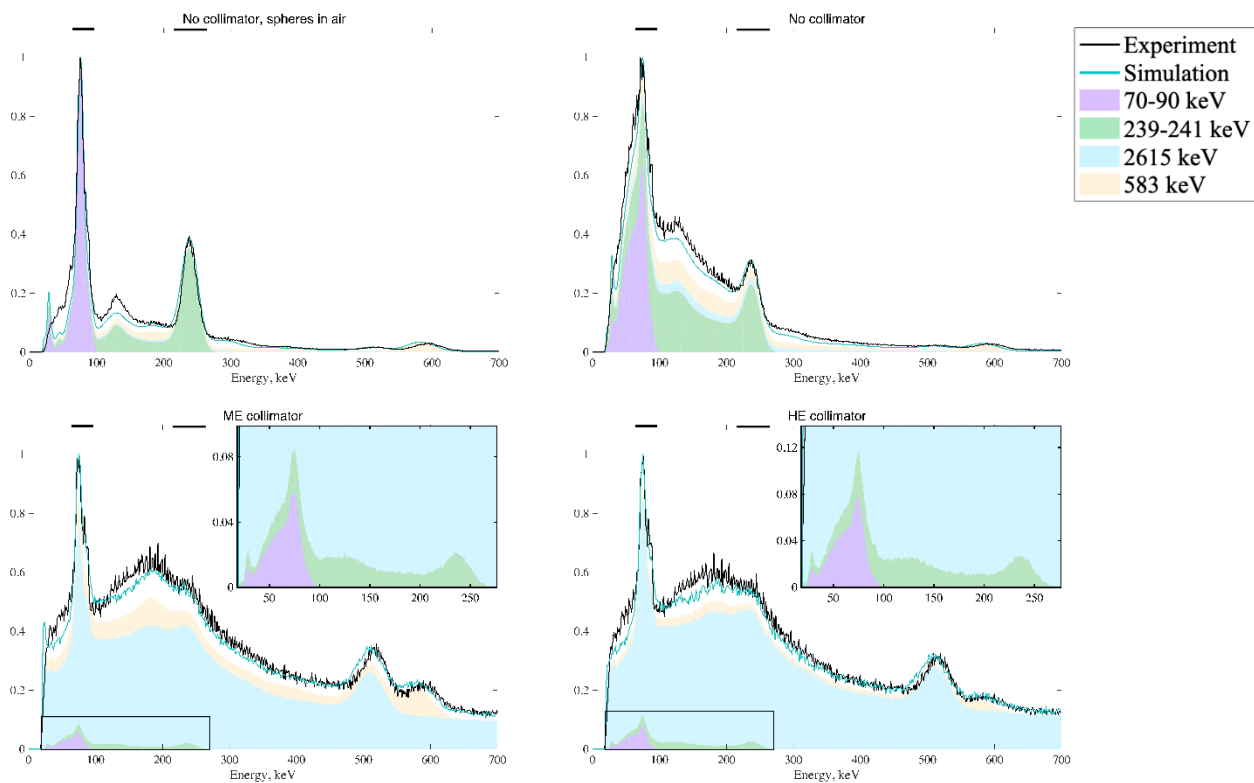
Updates	Iteration	Subset	Updates	Iteration	Subset	Updates	Iteration	Subset
5	=	5 × 1	34	=	17 × 2	240	=	30 × 8
6	=	6 × 1	38	=	19 × 2	300	=	30 × 10
8	=	8 × 1	42	=	21 × 2	360	=	30 × 12
10	=	10 × 1	45	=	15 × 3	450	=	30 × 15
12	=	12 × 1	60	=	30 × 2	600	=	30 × 20
16	=	16 × 1	75	=	25 × 3	720	=	30 × 24
20	=	20 × 1	90	=	30 × 3	900	=	30 × 30
24	=	24 × 1	120	=	30 × 4			
30	=	30 × 1	180	=	30 × 6			

Number of iterations and subsets used for each total number of Flash3D updates performed at reconstruction. 30 was the maximum number of iterations and subsets allowed.

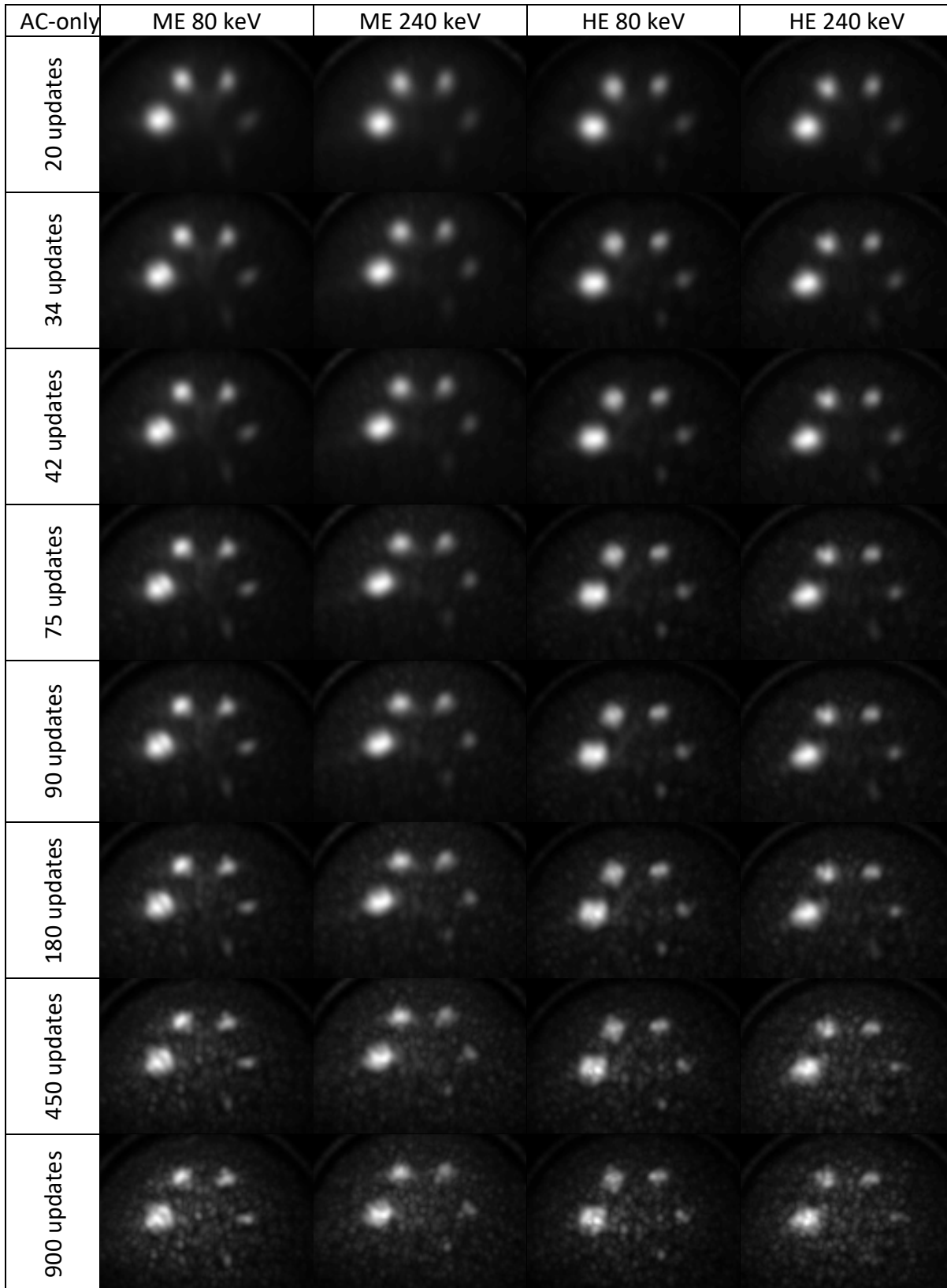
Supplemental Table 2: Overview of acquisitions, counts and scatter- to emission window count rate ratios (adjusted for window width).

Collimator	Energy window	Scan Duration [min]	Concentration [kBq/ml]	Total sphere Activity [MBq]	Primary window count rate [kCts / MBq·min]	Primary window counts [MCts]	Lower scatter window counts [MCts]	Upper scatter window counts [MCts]	Scatter window to emission window ratio
ME	80 keV	30	90	4,4	65.1	8.59	2.93	2.90	65.9 %
			30	1,4	73.4	3.08	1.05	1.04	65.7 %
	240 keV	30	90	4,4	75.7	10.0	2.79	2.06	90.9 %
			29	1,4	80.6	3.38	0.93	0.69	90.8 %
			3	20	0,9	109.2	0.29	0.08	0.06
HE	80 keV	30	95	4,6	37.8	4.80	1.67	1.62	66.5 %
			29	1,4	38.9	1.64	0.56	0.55	65.9 %
	240 keV		94	4,6	40.4	5.58	1.50	1.13	89.1 %
			29	1,4	43.1	1.81	0.49	0.37	89.1 %

Supplemental Figures

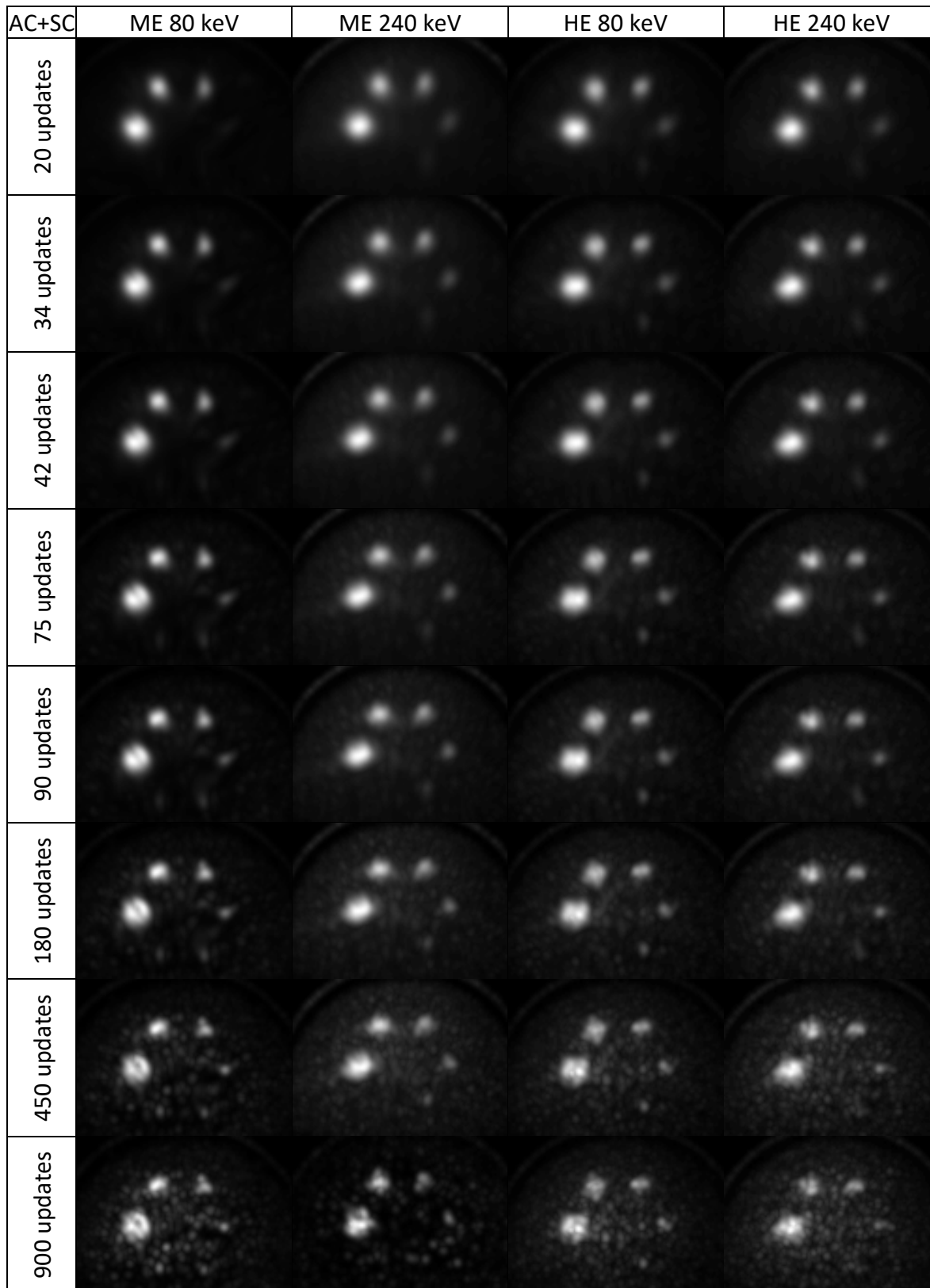


Supplemental Figure 1: Captured (black line) and Monte Carlo simulated (cyan line) energy spectra for different collimator configurations: Without (top), with ME (bottom left), and HE (bottom right) collimator. The energy windows are marked with black lines on the top axis. The contributions of selected emission photons (including simulated measurement uncertainty and lower energy secondary photons from these sources) is shown in the stacked histogram underneath: Photons emitted within the desired x-ray range (purple) and gamma rays (green), as well as 2615 keV (blue) and 583 keV (yellow) emissions, which cause low energy photon buildup following Compton Scatter, pair production and excitation of the lead collimators (x-rays). The desired signal photons provide strong peaks when measured without attenuating material or collimators (top left). When submerged in water Compton scatter from medium energy photons builds up (top right). The presence of collimators greatly increased secondary photons, and only a low percentage of captured counts are from the desired primary emissions in the clinically relevant setups (lower row); these contributions are shown enlarged in the top right boxes within the panels. The remaining white region of the stacked histograms consists of photons resulting from all other emissions.



Supplemental Figure 2: Transaxial maximum intensity projections (MIP) from acquisitions at 30 kBq/ml cropped around the phantom sphere inserts. Acquisitions were performed using the medium energy collimator (ME) and

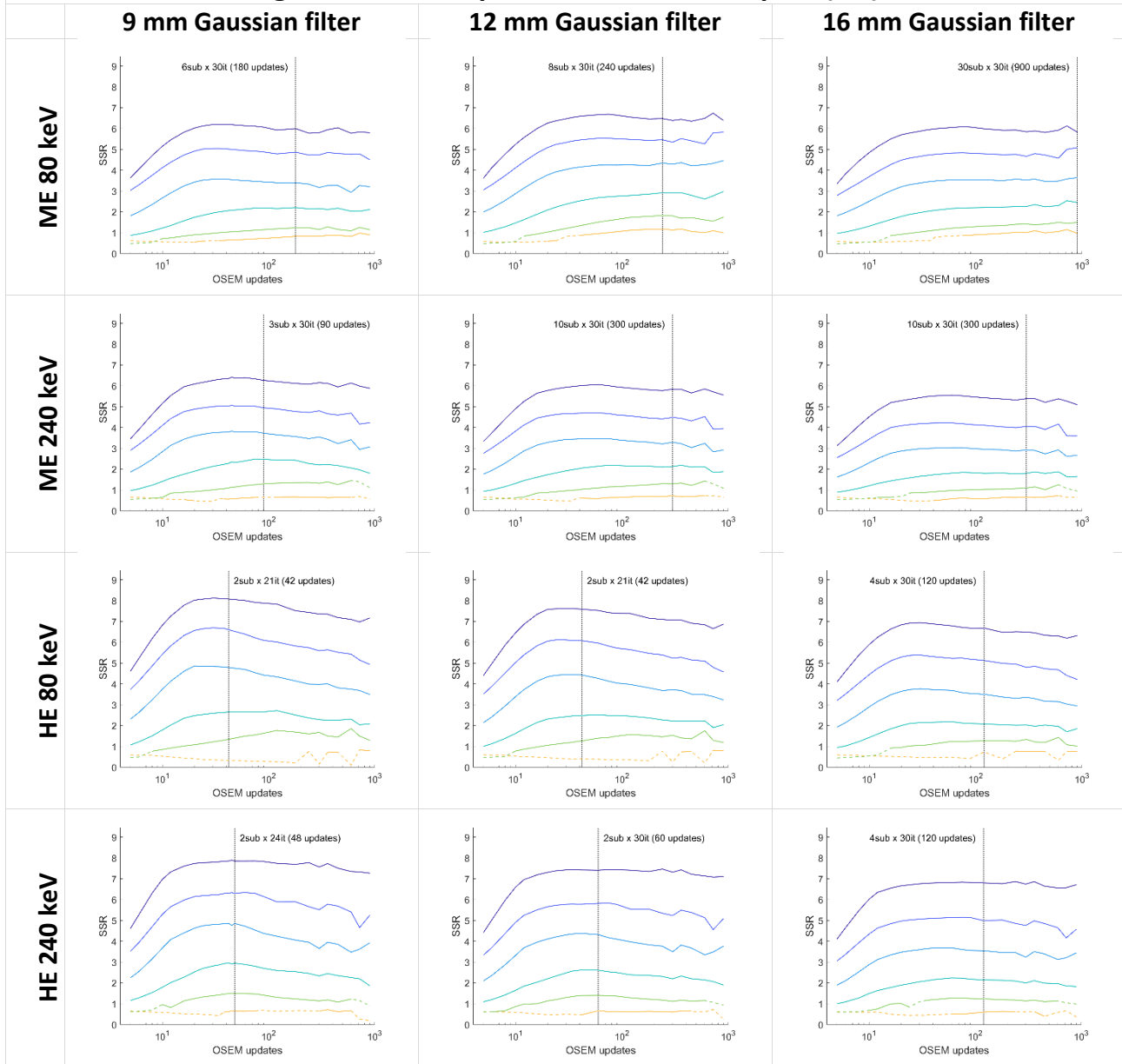
high energy collimator (HE); using windows centered around 80 and 240 keV. Reconstructions were performed using attenuation correction only, and post filtered with a 9 mm Gaussian filter. (Color: Linear gray scale from 0 to maximum intensity value.)



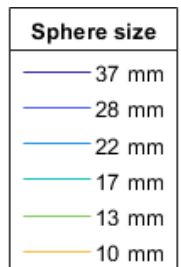
Supplemental Figure 3: Transaxial maximum intensity projections (MIP) from acquisitions at 30 kBq/ml cropped around the phantom sphere inserts. Acquisitions were performed using the medium energy collimator (ME) and

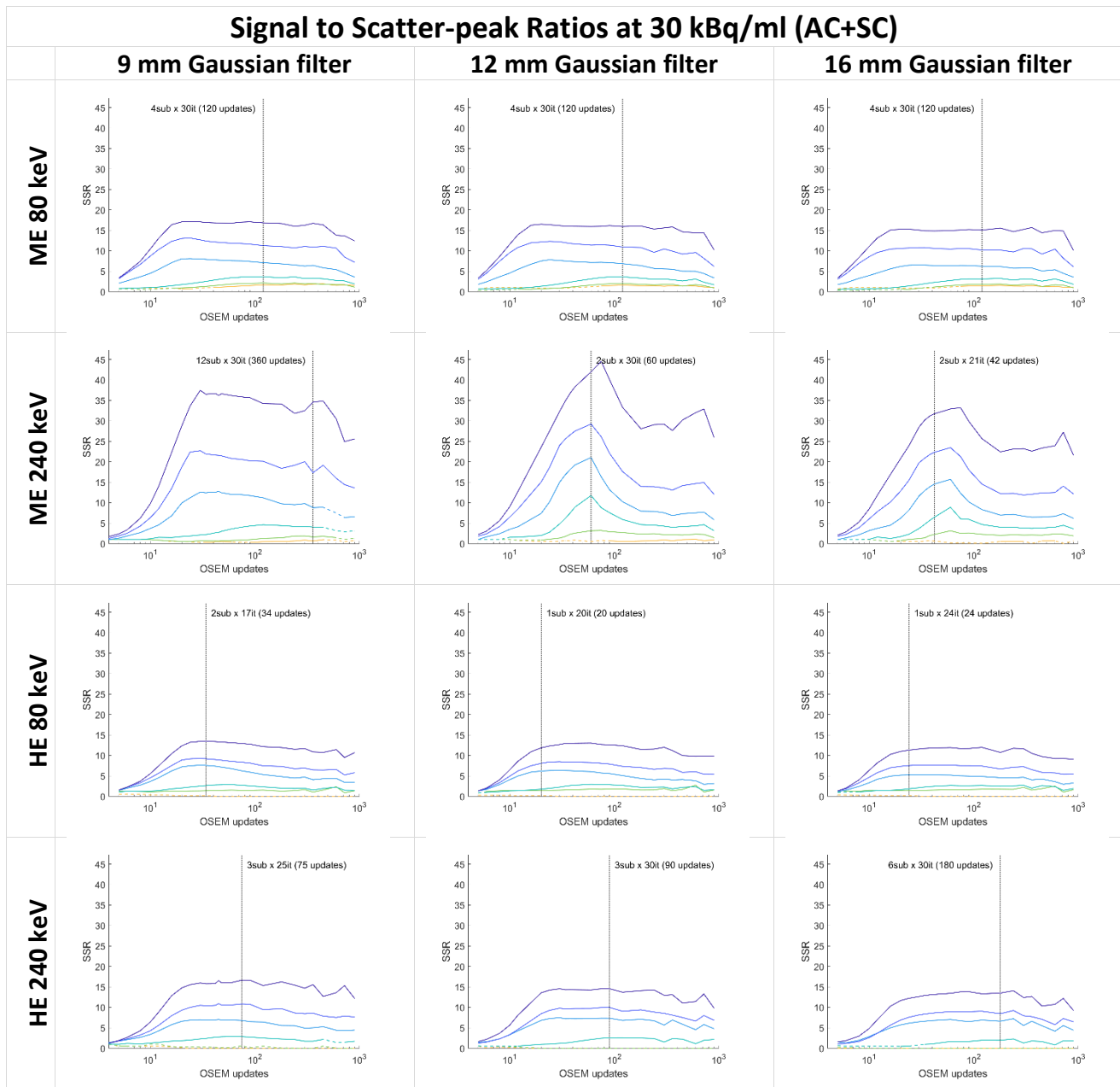
high energy collimator (HE); using windows centered around 80 and 240 keV. Reconstructions were performed using attenuation- and scatter correction at the indicated number of updates (rows) with 9 mm Gaussian post filter. (Colormap: Linear gray scale from 0 to maximum intensity value.)

Signal to Scatter-peak Ratios at 30 kBq/ml (AC)

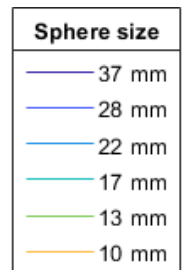


Supplemental Figure 4: Signal to scatter-peak ratios with 30 kBq/ml in the phantom, as a function of OSEM iterative updates (iterations × subsets), for each sphere in the phantom, for four different acquisitions (Medium Energy (ME) or High Energy (HE) collimator; 80 keV window or 240 keV window), reconstructed using attenuation correction (no scatter correction) and three different Gaussian post filtering strengths (9, 12 and 16 mm). The optimal iteration level (maximized total normalized SSR) is shown with a vertical line.

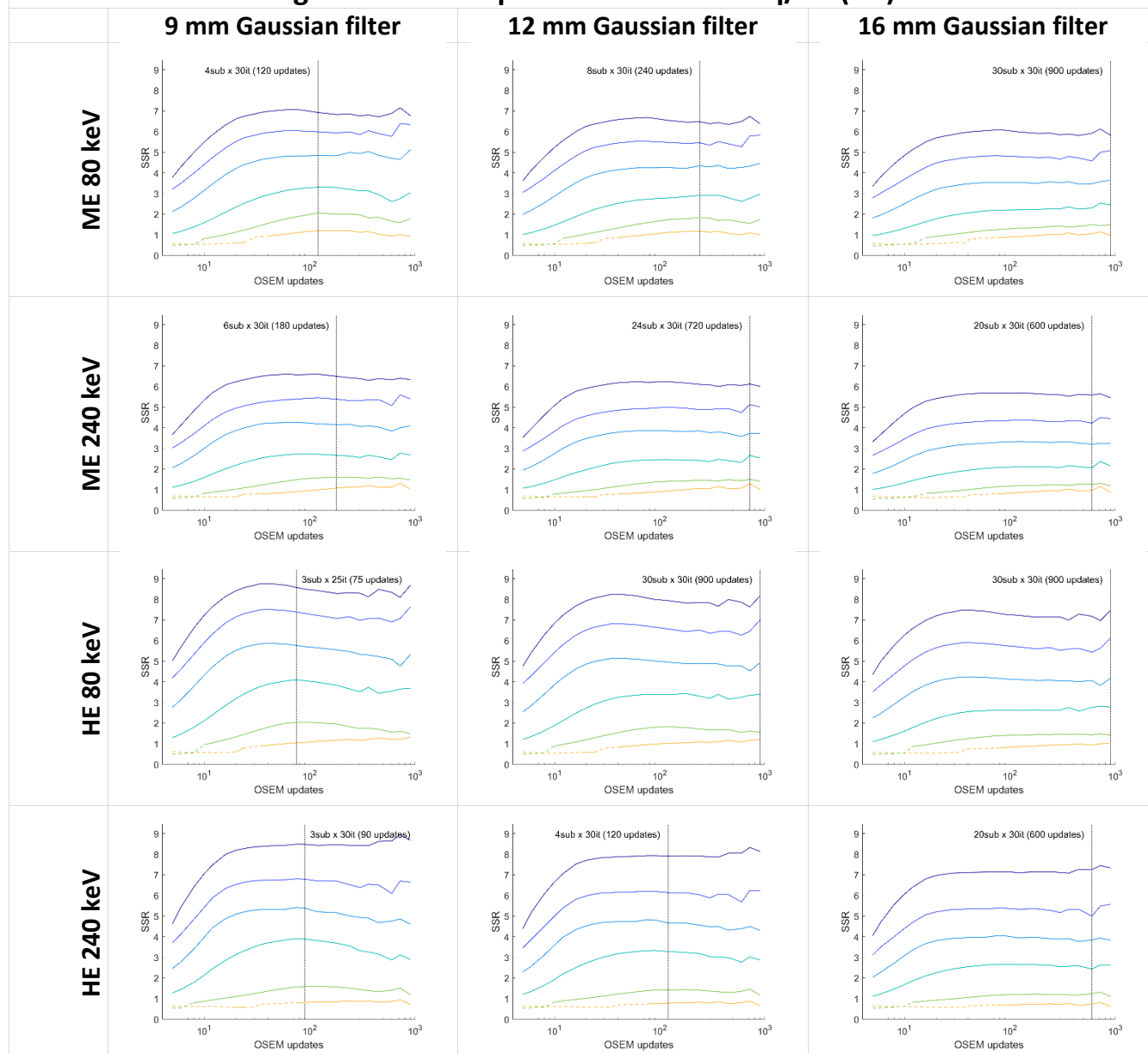




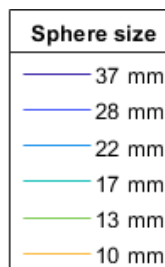
Supplemental Figure 5: Signal to scatter-peak ratios with 30 kBq/ml in the phantom, as a function of OSEM iterative updates (iterations × subsets), for each sphere in the phantom, for four different acquisitions (Medium Energy (ME) or High Energy (HE) collimator; 80 keV window or 240 keV window), reconstructed using attenuation correction and scatter correction (AC+SC) and three different Gaussian post filtering strengths (9, 12 and 16 mm). The SSR values are much greater using scatter correction and are plotted on a much wider scale, but lower than at 90 kBq/ml concentration.

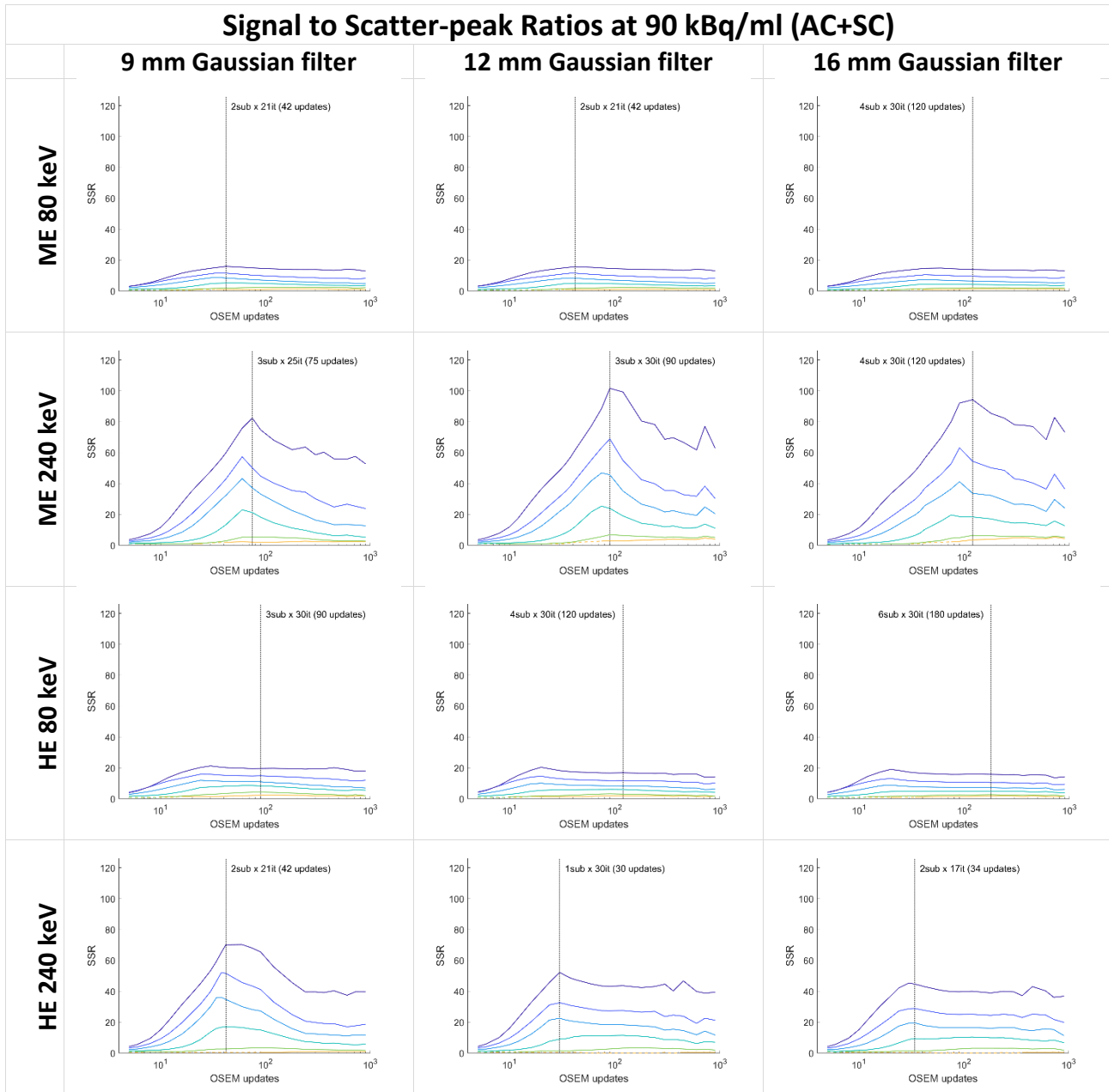


Signal to Scatter-peak Ratios at 90 kBq/ml (AC)

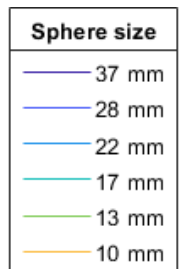


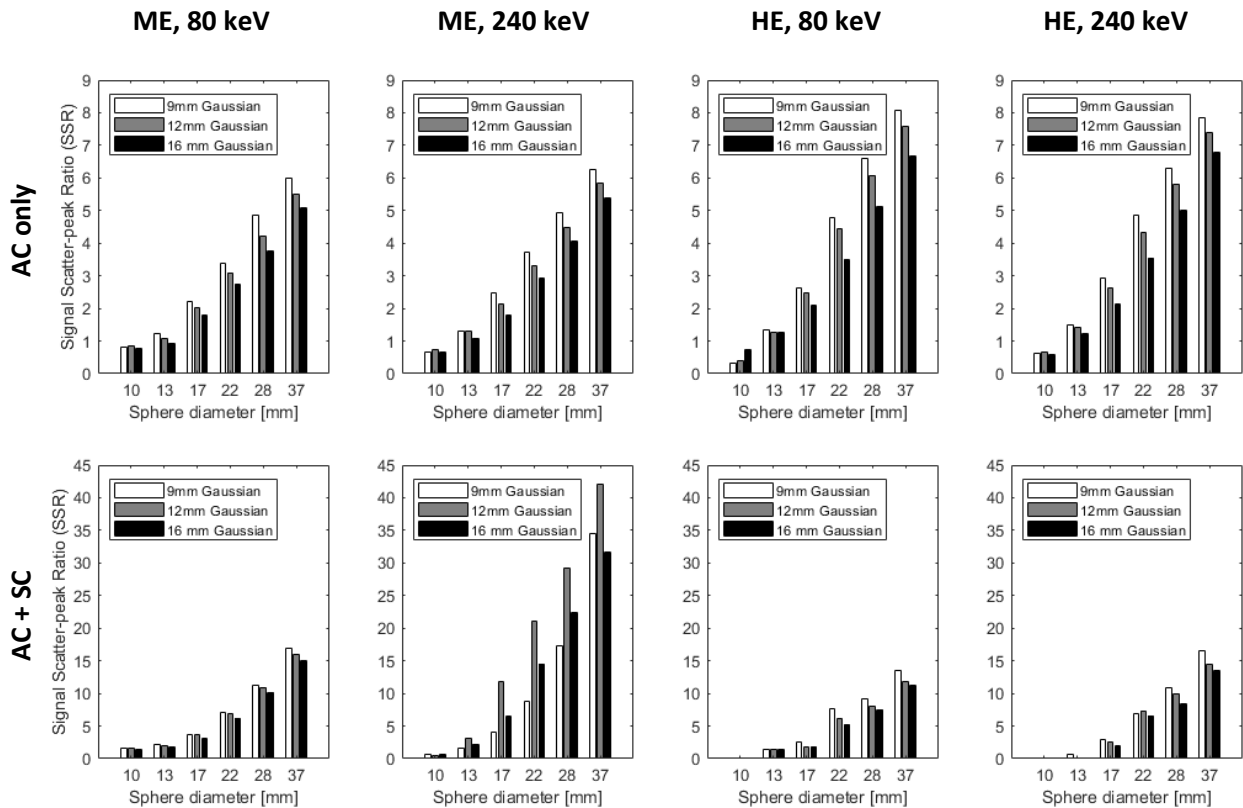
Supplemental Figure 6: Signal to scatter-peak ratios with 90 kBq/ml in the phantom, as a function of OSEM iterative updates (iterations × subsets), for each sphere in the phantom, for four different acquisitions (Medium Energy (ME) or High Energy (HE) collimator; 80 keV window or 240 keV window), reconstructed using attenuation correction (no scatter correction) and three different Gaussian post filtering strengths (9, 12 and 16 mm).



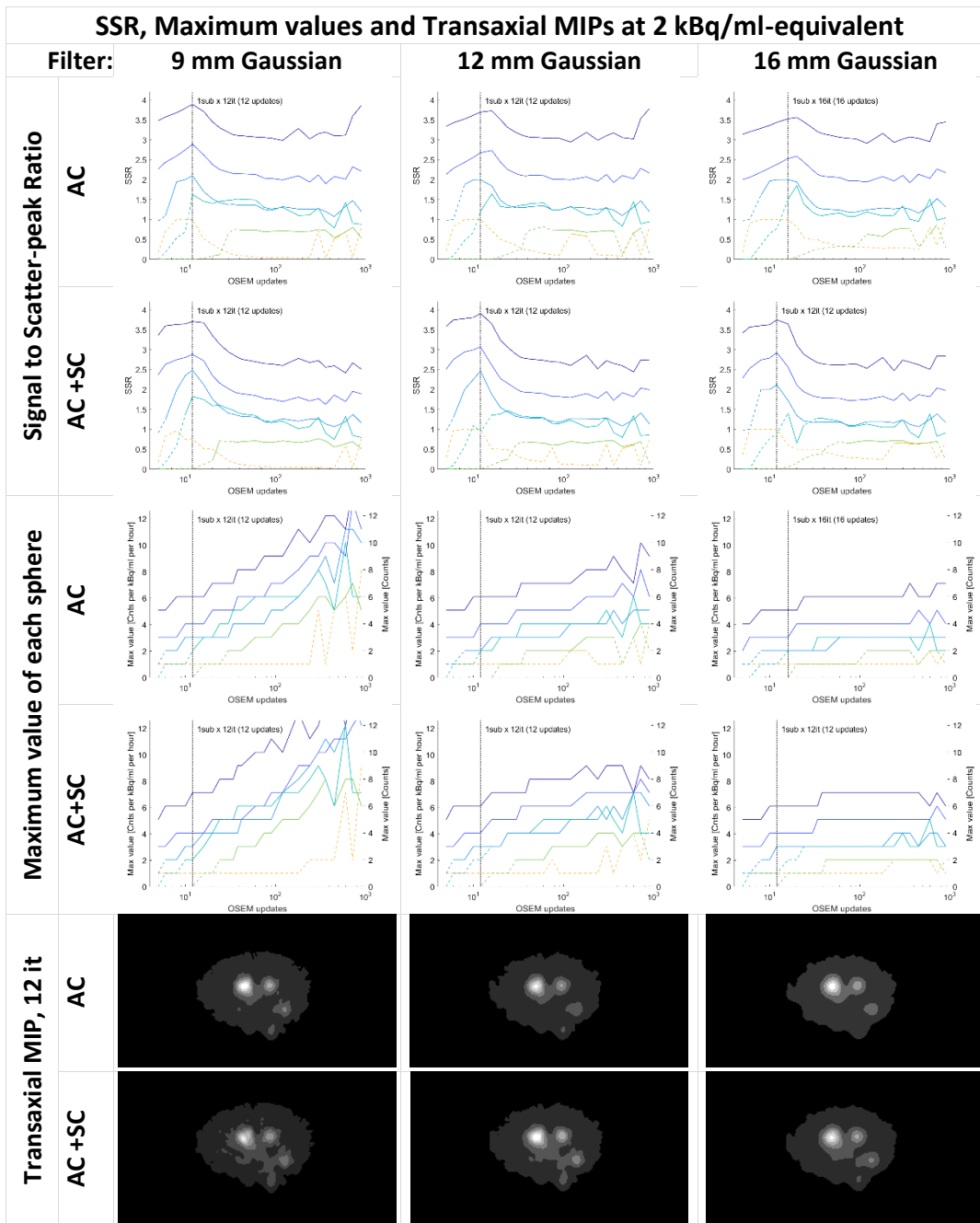


Supplemental Figure 7: Signal to scatter-peak ratios with 90 kBq/ml in the phantom, as a function of OSEM iterative updates (iterations \times subsets), for each sphere in the phantom, for four different acquisitions (Medium Energy (ME) or High Energy (HE) collimator; 80 keV window or 240 keV window), reconstructed using attenuation correction and scatter correction (AC+SC) and three different Gaussian post filtering strengths (9, 12 and 16 mm). The SSR values are much greater using scatter correction and are plotted on a much wider scale.

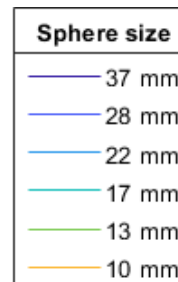


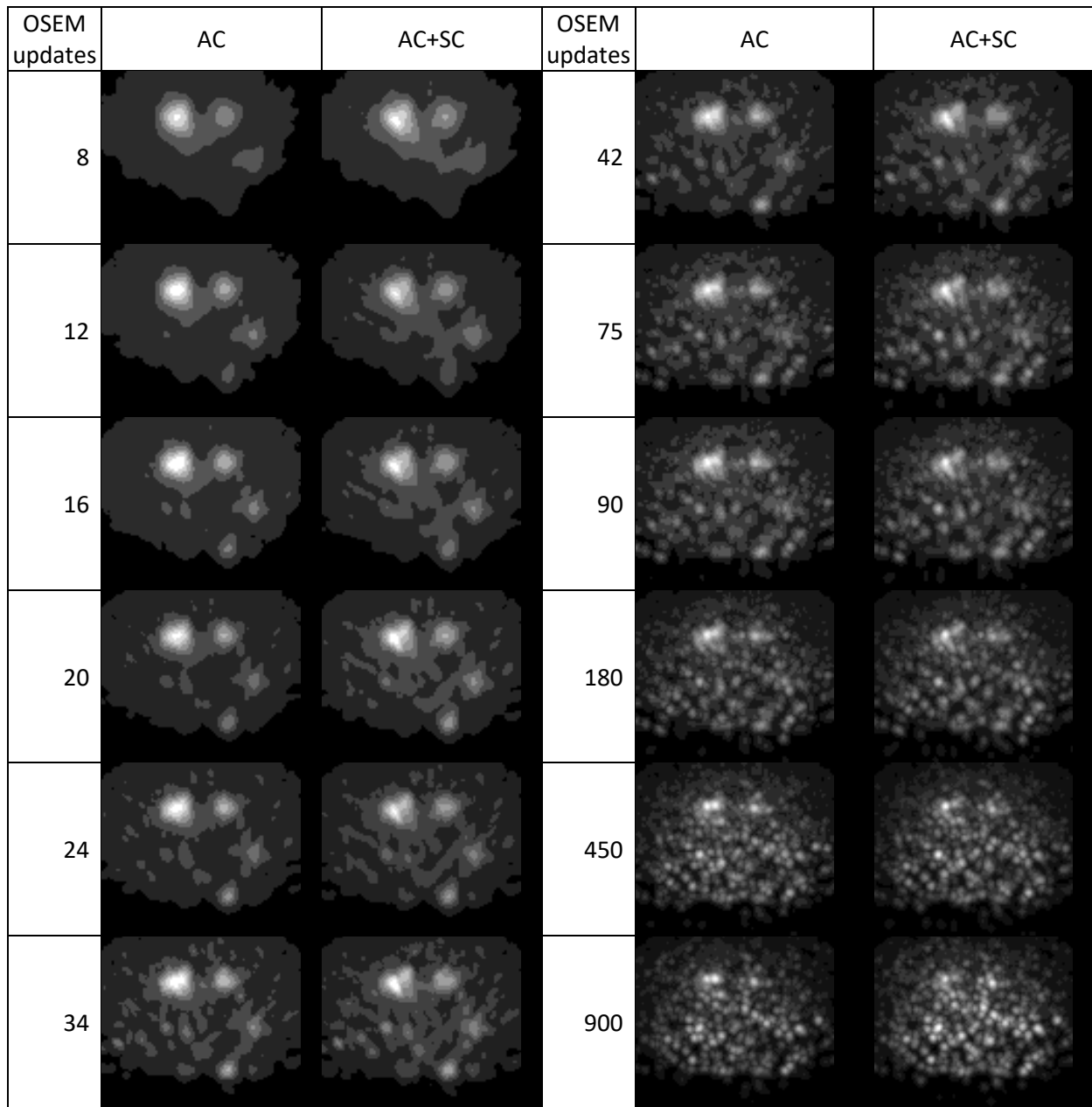


Supplemental Figure 8: Effects on SSR from post filter strength. Top row: Attenuation correction only;; lower row, attenuation and scatter corrected reconstructions. Panels left to right, Medium energy collimator (ME) at 80 and 240 keV windows, followed by high energy collimator (HE) at 80 and 240 keV windows. Bars are grouped left to right according to sphere sizes, and within each group the SSR obtained with 9, 12 and 16 mm Gaussian post filter is shown from left to right. The SSR values are from the iterative reconstruction with the optimal number of updates for each of the displayed acquisition/window/correction configurations. Y-axis scale is the same within each row, but scatter corrected data is displayed at a five times wider scale.

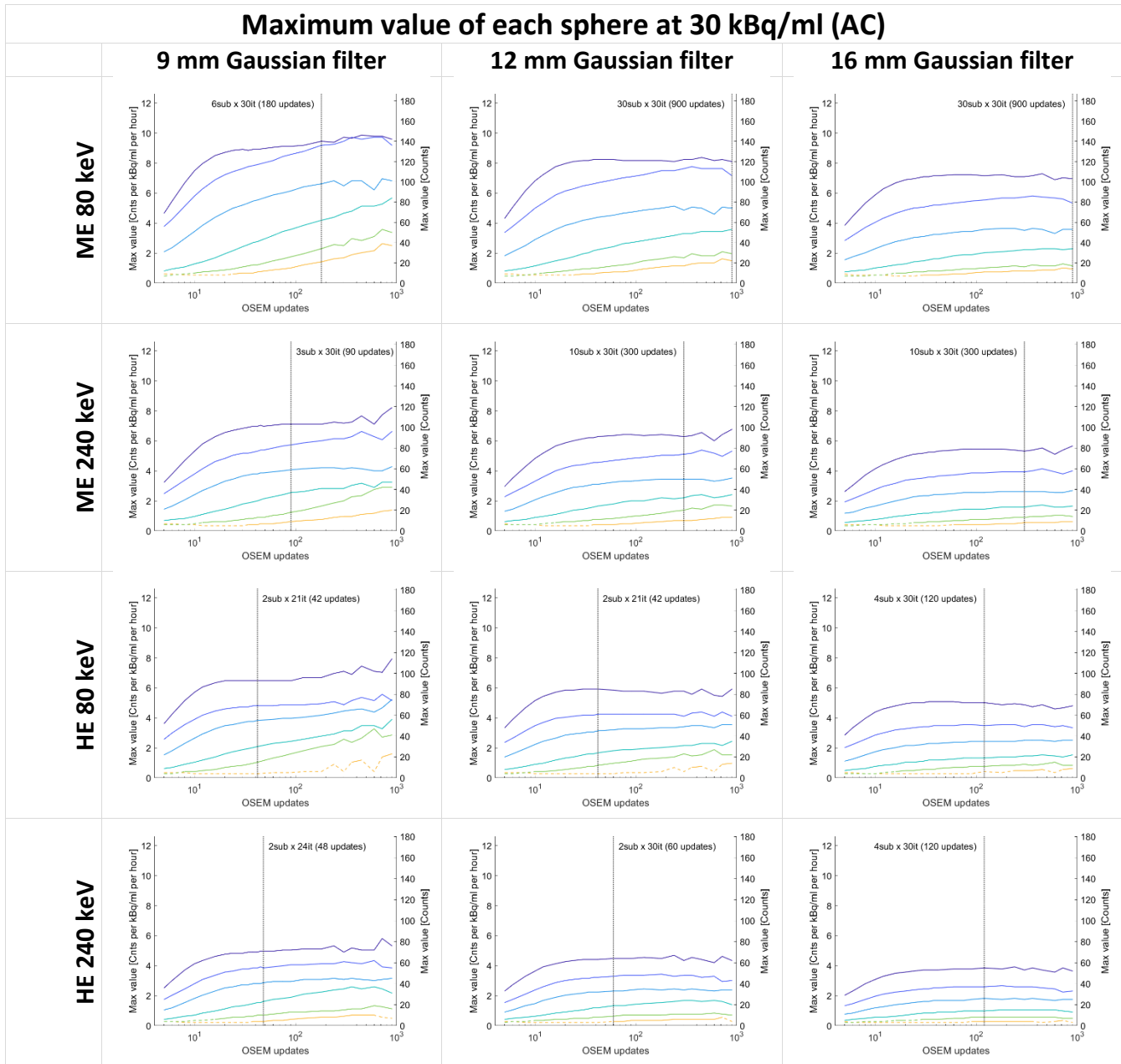


Supplemental Figure 9: Results from the 3 minute scan at 20 kBq/ml (equivalent to 2 kBq/ml). Columns: Different Gaussian post processing filter strengths. Rows show Signal to scatter-peak ratio (SSR); Sphere maximum normalized countrate (left axis) and absolute value (right axis); and a transaxial Maximum intensity projection (MIP) captured at the optimal OSEM iterative level according to SSR (12 iterations, 1 subset). Every other row show reconstructions using attenuation correction only (AC) and attenuation plus scatter correction (AC+SC). (Colormap: Linear gray scale from 0 to maximum intensity value.)

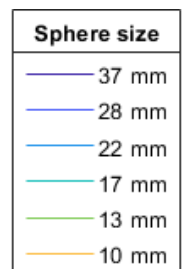


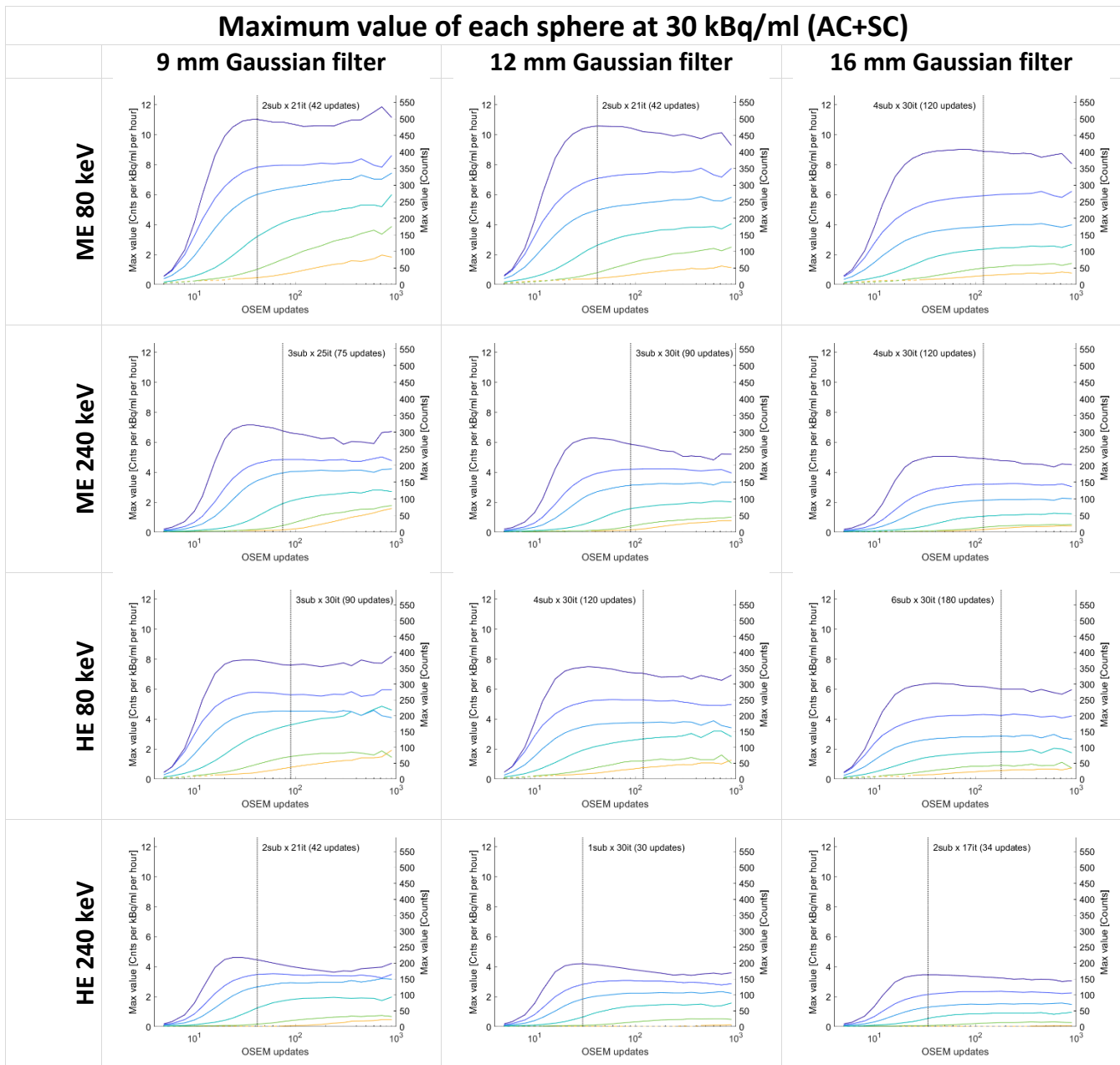


Supplemental Figure 10: Comparison of reconstructed transaxial maximum intensity projections of the 2 kBq/ml-equivalent acquisition, reconstructed using 9 mm Gaussian postprocessing filter, and either attenuation correction only (AC) or attenuation and scatter correction (AC+SC). (Colormap: Linear gray scale from 0 to maximum intensity value.)

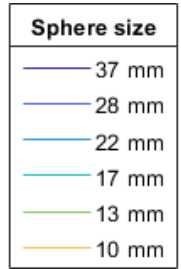


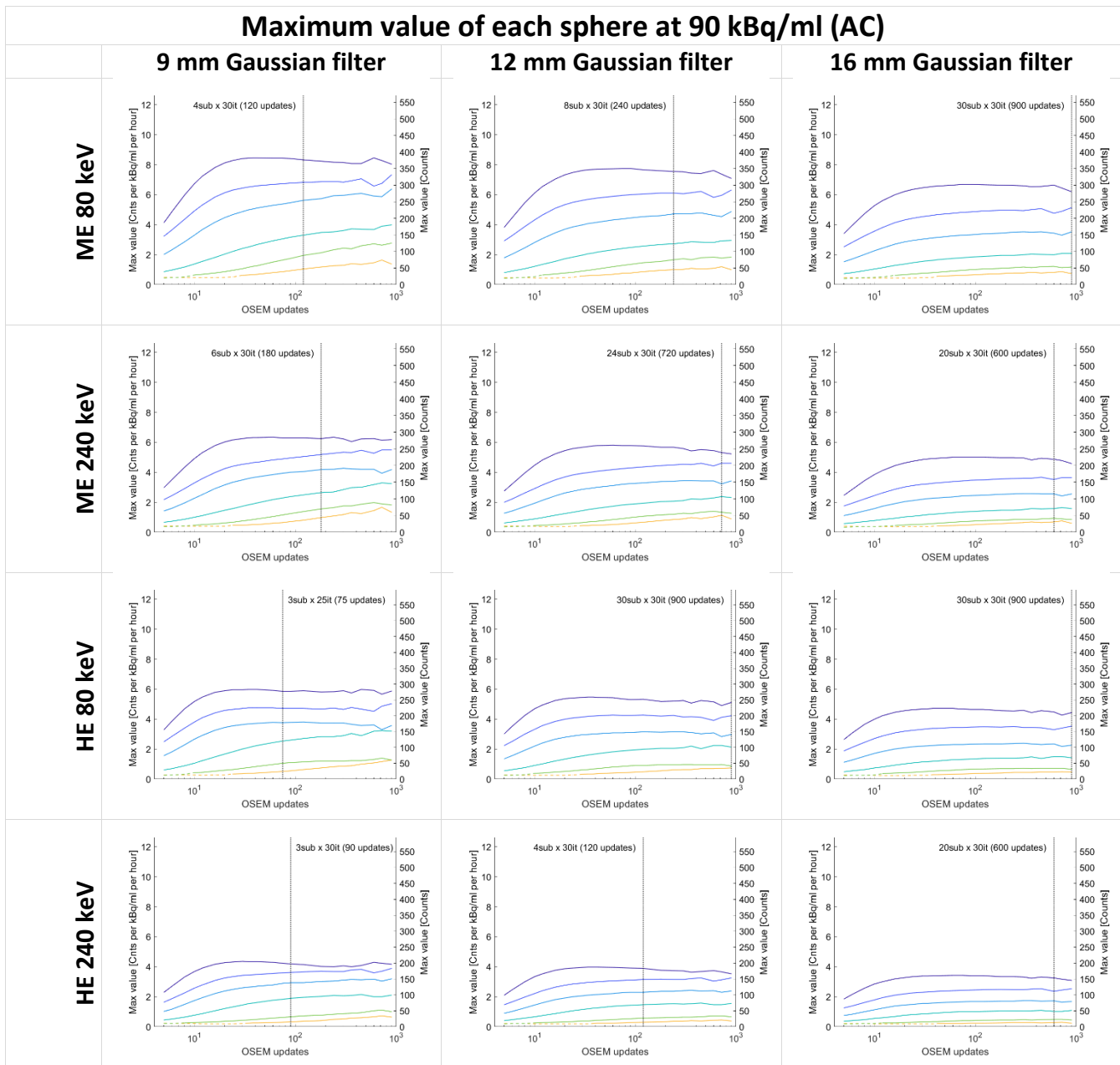
Supplemental Figure 11: Maximum normalized count rate (left y-axis) and count value (right y-axis) of each sphere in the phantom captured at 30 kBq/ml. The panels show four different acquisitions (Medium Energy (ME) or High Energy (HE) collimator combined with 80 keV window or 240 keV window), reconstructed using attenuation correction (AC) only and three different Gaussian post filtering strengths (9, 12 and 16 mm).



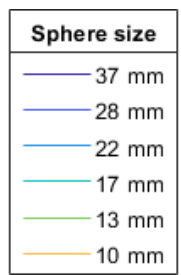


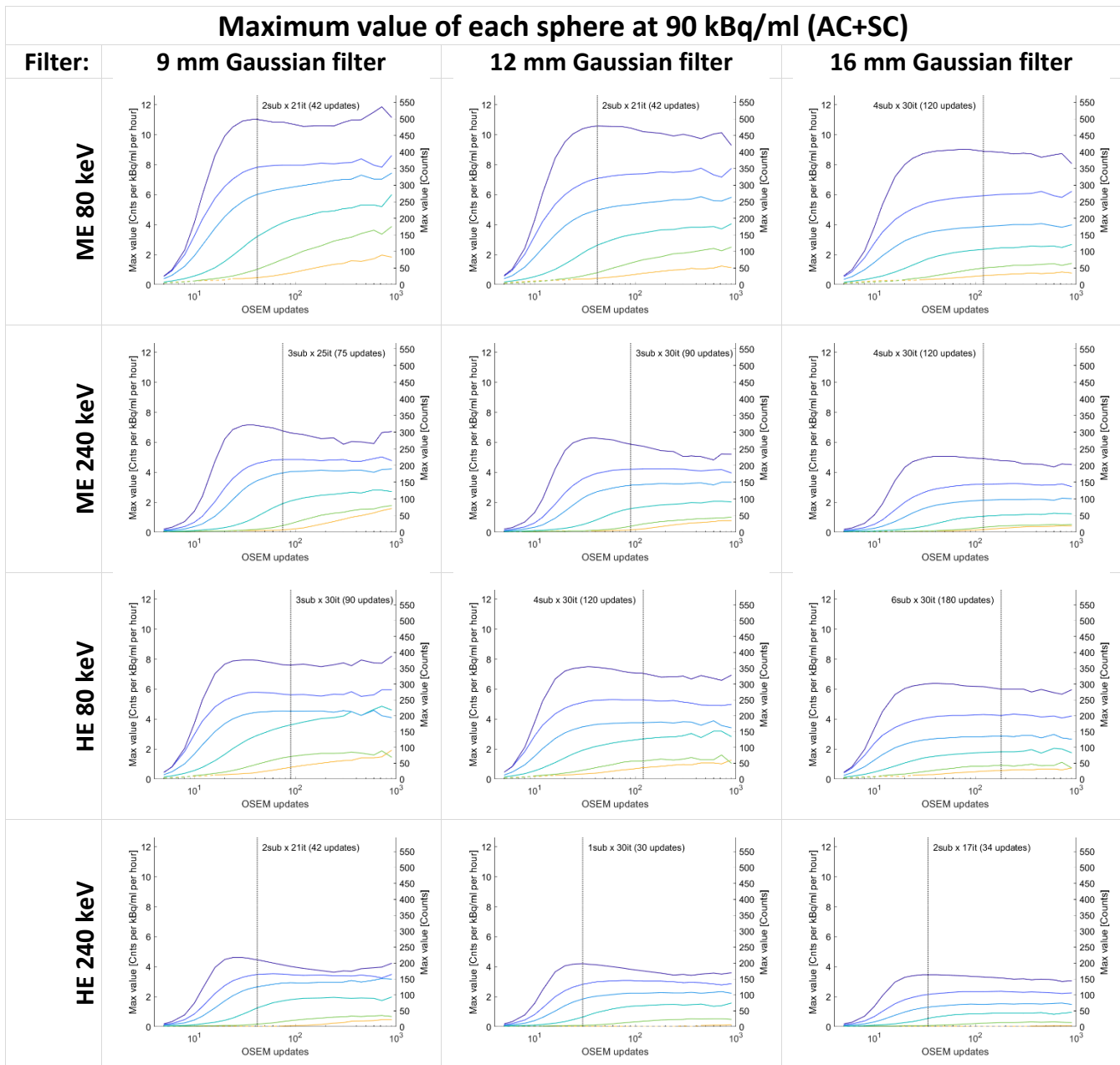
Supplemental Figure 12: Maximum normalized count rate (left y-axis) and count value (right y-axis) of each sphere in the phantom captured at 90 kBq/ml. The panels show four different acquisitions (Medium Energy (ME) or High Energy (HE) collimator combined with 80 keV window or 240 keV window), reconstructed using attenuation correction and scatter correction (AC+SC) and three different Gaussian post filtering strengths (9, 12 and 16 mm).



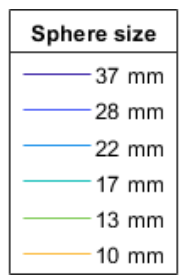


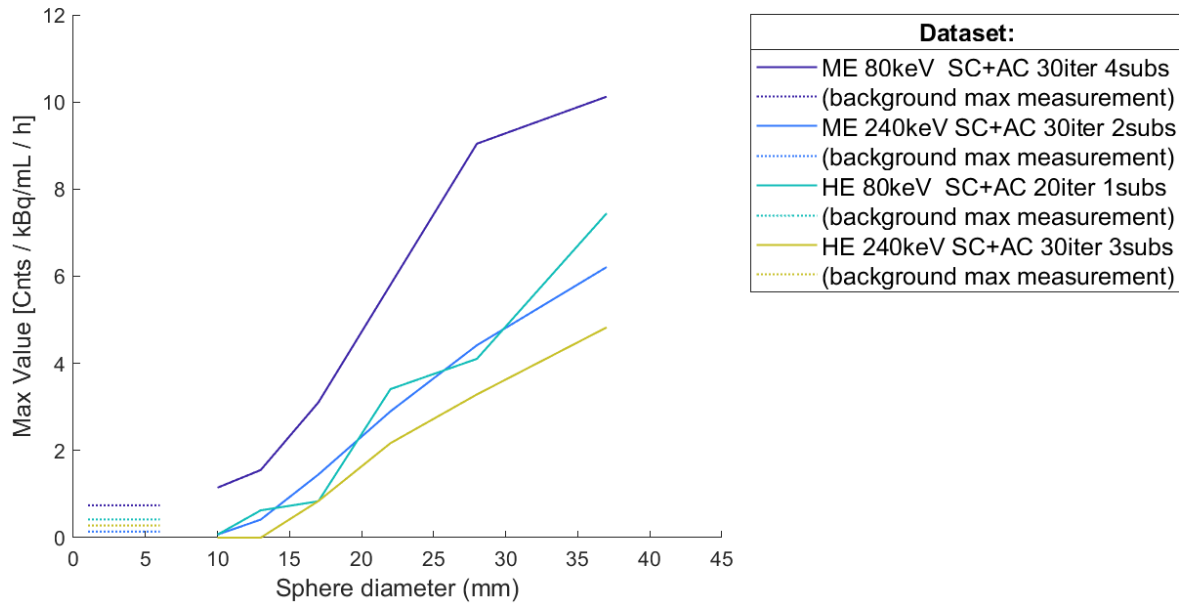
Supplemental Figure 13: Maximum normalized countrate (left y-axis) and count value (right y-axis) of each sphere in the phantom captured at 90 kBq/ml. The panels show four different acquisitions (Medium Energy (ME) or High Energy (HE) collimator combined with 80 keV window or 240 keV window), reconstructed using attenuation correction (AC) only and three different Gaussian post filtering strengths (9, 12 and 16 mm).





Supplemental Figure 14: Maximum normalized countrate (left y-axis) and count value (right y-axis) of each sphere in the phantom captured at 90 kBq/ml. The panels show four different acquisitions (Medium Energy (ME) or High Energy (HE) collimator combined with 80 keV window or 240 keV window), reconstructed using attenuation correction and scatter correction (AC+SC) and three different Gaussian post filtering strengths (9, 12 and 16 mm).





Supplemental Figure 15: Absolute Resolution Recovery of each collimator and energy window acquisition captured at approximately 30 kBq/ml. The maximum value of the background region of interest is shown in dotted lines to the left. Only scatter + attenuation corrected data is showed. The number of iterations and subsets used in the various reconstructions are noted in the legend.